JOURNAL OF MATERIALS SCIENCE 26 (1991) 4774–4786

Organic photoconductors: Dark and photoconduction studies in two p-dimethylamino styryl dyes derived from pyridine-2 and pyridine-4

P. K. NARASIMHARAGHAVAN*, HARI OM YADAV, T. S. VARADARAJAN
Centre for Advanced Studies in Applied Chemistry, Department of Chemical Technology, University of Bombay, Matunga, Bombay 400 019, India

L. N. PATNAIK, S. DAS
Department of Chemistry, Ravenshaw College, Cuttack 753 003, India

Results of our experiments on the dark and photoconduction studies in two p-dimethylamino styryl dyes derived from pyridine-2 (PDMS-P2) and pyridine-4 (PDMS-P4) in their pure form without any dopant or additive are reported. Measurements on surface-type (raster pattern) cells show that the dark and photocurrents are dependent on the applied potential, temperature, and the photocurrent on the intensity of the incident radiation and the wavelength. Action spectra of the samples could not be recorded as the intensity of the monochromatic radiation from the monochromator reaching the sample was too low to induce any noticeable photocurrent. The compounds show a low dark conductivity. The dark and photocurrents show a perfect ohmic behaviour in the temperature range studied (288–328 K). Since photoconduction could only be observed in a vacuum, this clearly indicates that the compounds are n-type semiconductors. The observed rise and decay kinetics of the photocurrents indicate the presence of traps in the forbidden zone. The dyes show an enhanced photoconduction on illumination with visible radiation only. The marked open circuit voltage and the short-circuit current observed in these compounds indicate a possible application in solar photovoltaics.

1. Introduction

Two factors which are essential for a material to be a good photoconductor are high absorption in the visible spectrum and chemical stability. Recently there has been an increased interest on the organic pigments, especially the phthalocyanines [1–4], which are characterised by a variety of colorant and non-colorant properties, and the cyanine dyes [5] for their possible applicaton in memory devices. The possible application of phthalocyanine derivatives (as catalysts in fuel cell cathodes [6], as photoconductors in photoelectrochemical solar cells [7, 8], as xerographic photoreceptors, and as vedicon television pickup tubes [2, 9]) makes it a potential candidate for future research. However, the photoelectric sensitivity of the phthalocyanines may be restricted by a low probability of the photogeneration of the free carriers as a result of a small Onsager distance [10]. Therefore, the power conversion efficiencies of the phthalocyanine photovoltaic devices probably cannot approach those of the inorganic semiconductors [11–14].

Because efficiencies of the order of 10% may not be excluded in organic solar cells by any theoretical means [2, 15–18], systematic studies of various compounds are necessary. It is hoped that such studies would provide further insight to the principles governing the charge carrier generation process and the carrier transport properties of the organic molecular solids which can be considered as candidates for use in photovoltaic devices.

A potential candidate in this line would be the cationic dyes which have been explored for their application as photosensitizers [19–21], photoconductors [22–24] and as solar photovoltaics [27, 28]. The aim of these studies was to produce a simple and inexpensive solar cell having conversion efficiencies nearer to the theoretically predicted value (10%). As mentioned earlier, a proper understanding of the nature of the processes leading to the observed dark and photoconduction in these compounds is lacking at the present time.

Usually, the spectral sensitivity of the photoconductors is measured by the discharge of surface charge on the film using the xerographic method [29]. The sensitivity is expressed as the reciprocal of the exposure energy for a half discharge. This method does not

* Author to whom all correspondence should be addressed: presently c/o V. A. Kuzmin, Institute of Chemical Physics, USSR Academy of Sciences, 4, Kasigen Street, Moscow-117334, USSR.

0022–2461/91 $03.00 + .12

seem to include the photoconduction process, but only the carrier generation process, because, the carrier transport takes place near the irradiated region. A high absorption coefficient suggests that the carrier generation layer is very thin. Then the photoconduction process is almost totally controlled by the non-irradiated high-resistive region. Therefore, the photocurrent is strongly dependent on the absorption coefficient and the film thickness. This problem can be overcome to some extent by using a surface-type raster cell arrangement [30].

Certain donar-acceptor molecules, such as dimethylamino benzonitrile (DMBN), exhibit a peculiar twisted internal charge transfer state (TICT) [31–33]. In the ground state, the molecule is planar due to the conjugation between the lone pair nitrogen of the dimethylamino group and the benzonitrile cycle. The excitations in the charge transfer band gives rise to a planar excited state with a weak dipolar character by a vertical (Frank-Condon) process.

The occurrence of this twisting process appears attractive for molecular switches, since there is an almost perfect orbital decoupling in the TICT state. We consider that the coordination complexes containing redox sites linked to this kind of molecule could be a good model for testing the possibility of molecular switches. The DMBN and its derivatives can be used as ligands through their nitrile end and J. P. Launary *et al.* [34] have suggested that some peculiar photophysical properties may exist in these complexes.

Patnaik and Das [35] have studied the structural conformation and stability of PDMS-P2 and PDMS-P4 and have developed a theory based on the results obtained from the above mentioned study on the basis of perturbative configuration interaction using localised orbitals (so-called PCILO method). They have also reported similar twisted states in these compounds.

In this paper we report the first results of the studies of dark and photoconduction studies in PDMS-P2 and PDMS-P4 without any dopant or additive. The structure and the electron flow in these compounds are shown in Fig. 1. It is a part of our investigations on the conductivity of cationic styryl dyes derived from different heterocyclic nuclei. The studies have been carried out with an aim of finding out any possible structure-semiconductivity relationship that would aid the design and synthesis of dyes with prefixed semiconducting properties.

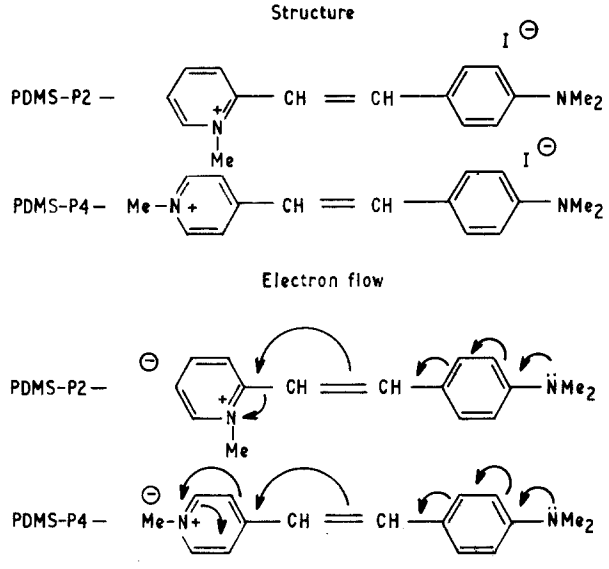

Figure 1 The structure and the electron flow in PDMS-P2 and PDMS-P4. The flow of electron (intra-Molecular) is shown by arrows.

2. Experimental details

The two p-dimethylamino styryl dyes, PDMS-P2 and PDMS-P4, kindly supplied by L. N. Patnaik in their purest form (column chromatographed), were used without any further purification. Surface-type raster cells employing silver paste contacts with electrode distance of 0.02 cm have been used for studying the electrical properties. This is shown schematically in Fig. 2. The raster cell has 35 gaps and the inter-electrode distance was maintained at 0.02 cm. The raster cell was prepared by photo-etching the aluminium coated (by vacuum sublimation at 10^{-4} torr) on carefully cleaned transparent quartz slides. The dye was sublimed at vacuum better than 10^{-4} torr on these gaps for the purpose of the conductivity measurements.

The samples were investigated under vacuum at $\sim 10^{-5}$ to 10^{-6} torr in the temperature range 288–328 K using an electrical heater. To avoid the backstreaming of the oil vapours, the oil diffusion pump was used in combination with a liquid nitrogen trap. The sample temperature could be maintained and measured to an accuracy of ± 0.5 K using a temperature indicator in combination with a temperature controller.

The construction of the condutivity set-up has been discussed elesewhere [36]. A schematic diagram of the experimental set-up (block diagram) showing the conductivity arrangement is shown in Fig. 3. Dark and photocurrents were registered with a digital picoammeter (Model EA5600, Electronic Corporation of India). In addition, the rise and decay kinetics of the photocurrent have been studied using the picoammeter in combination with a fast recorder.

The light source consisted of a 500 W xenon arc lamp (Kratos, West Germany) focused by a well defined system of quartz lenses on to the photoelectric

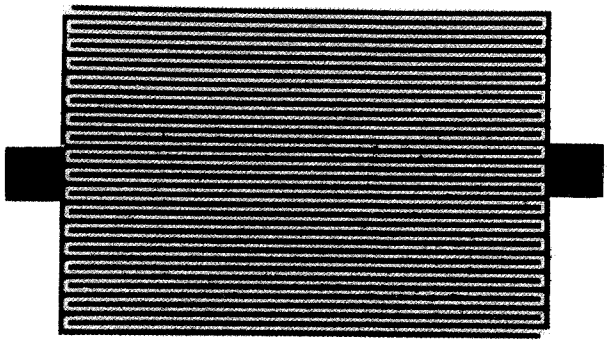

Figure 2 A Raster cell pattern (enlarged for convenience). The distance between the successive electrodes is 0.02 cm.

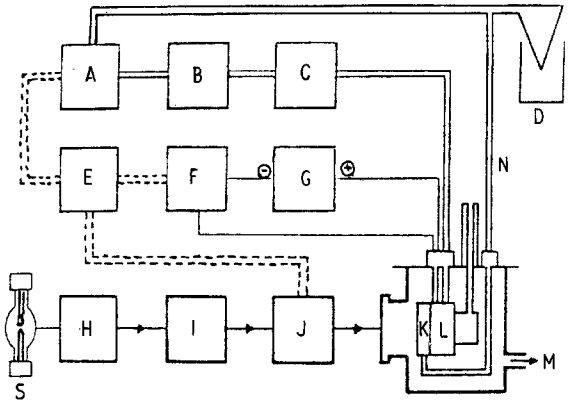

Figure 3 A schematic representation of the experimental set-up showing the different components. Key: (A) digital temperature indicator, (B) programmable temperature controller, (C) d.c. power supply to heater, (D) ice (reference temperature 0°C), (E) X-Y recorder, (F) digital picoammeter, (G) stabilized power supply, (H) condensing system, (I) water column, (J) monochromator or filters, (K) sample holder (with heater), (L) liquid nitrogen cylinder, (M) to vacuum pumping system, (N) thermocouple (temperature sensing), and (S) source (xenon arc lamp).

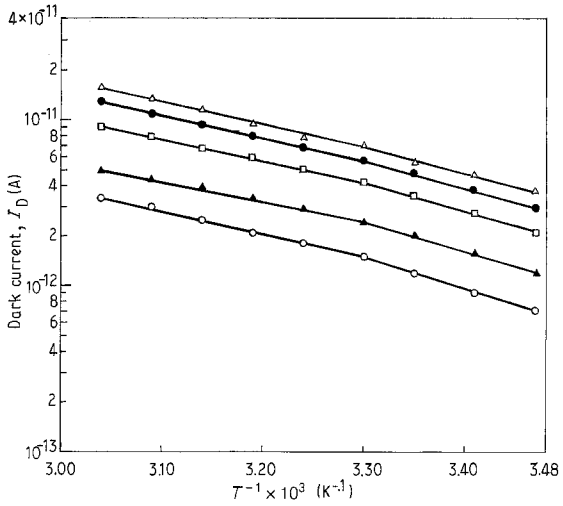

Figure 4 The temperature dependence of dark current of PDMS-P2 at 288 K < T < 328 K (surface-type raster cell arrangement) at different applied potentials: (○) 30, (▲) 50, (□) 90, (●) 120 and (△) 150 V.

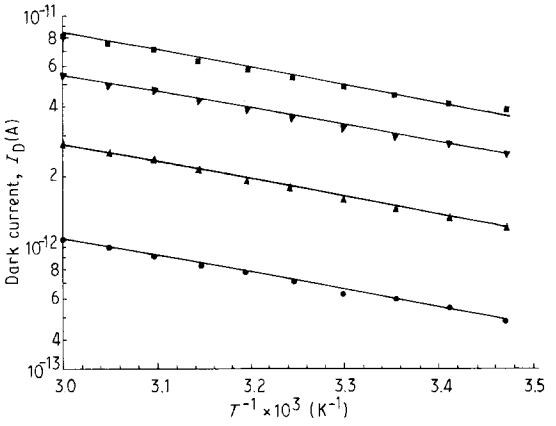

Figure 5 The temperature dependence of dark current of PDMS-P4 at 288 K < T < 328 K (surface-type raster cell arrangement) at different applied potentials: (●) 20, (▼) 50, (▲) 100, and (■) 150 V.

cell. A water column (a quartz cell containing distilled water) was used to filter out infra-red radiation from the lamp. Quartz neutral density filters were used for studying the intensity dependence of photoconduction. Home-made quartz neutral density filters were calibrated using a ultra-violet/visible spectrophotometer (Pye Unicam SP8000). Visible and u.v. radiation could be obtained separately from the lamp source by using u.v. and visible cut-off filters.

Out-gassing of the samples was carried out by cyclically heating and cooling the samples under vacuum conditions.

3. Results and discussion

3.1. Dark conductivity

The variation of dark current (I_D) with temperature, measured in the surface-type cells of PDMS-P2 and PDMS-P4, can be described by the equation

$$I_D = A \exp(-\Delta E_D/kT) \quad (1)$$

where k is the Boltzmann constant, T is the absolute temperature. A is the pre-exponential factor, and ΔE_D is the thermal activation energy of dark conduction. The parameters derived from the plots of the logarithm of dark current ($\log I_D$) against the reciprocal of the temperature (Figs 4 and 5) for the compounds are shown in Table I.

The increase in the dark current with increasing temperature corresponding to Equation 1, is typical for organic semiconductors [11, 30]. It may arise from a direct generation of the charge carrier across the energy gap (in the case of intrinsic semiconductors) or by an excitation of the donor or acceptor states (in the case of extrinsic or impurity semiconductors). The observed values of ΔE_D being very small, the possibility of ΔE_D being equal to the band gap is ruled out. No data are available on the ionization energy (I_C) and the electron affinity (A_C) of the compounds. Consequently, testing of the intrinsic nature of the compounds, for example, by comparing the ΔE_D values with the quantity $I_C - A_C$ [30] is not possible. Hence, it can be stated that the values ΔE_D merely give the depth of the traps from the conduction band from which the charge carriers are liberated during the thermal process.

The two activaton energies observed for PDMS-P2 may be explained as follows. In both the cases the conduction is extrinsic. The change of slope merely indicates a change from $\Delta E_D/kT$ in the lower temperature range to $\Delta E_D'/2kT$ in the higher temperature range, caused by a change in the number of excited carriers n, relative to the number of impurity levels N, where N is less than the total number of carriers N_e.

In this context, it is remarkable that the dark currents for PDMS-P2 and PDMS-P4 increase with increasing applied potential (Figs 6 and 7) according to the relation

$$I_D = aU^s \quad (2)$$

where U is the field, a is a constant and s is the power factor. From the logarithmic plot of the dark current

TABLE I Thermal activation energy of dark conduction (ΔE_D) and the activation energy of photoconduction (ΔE_{ph}) at different intensities of illuminations for PDMS-P2 and PDMS-P4

Compound	ΔE_D (eV)	ΔE_{ph} (eV)					
		100%	63%	52%	29%	Visible only	u.v. only
PDMS-P2	0.3278–0.3062 (288–303 K) 0.5146–0.6816 (303–328 K)	0.2943	0.2703	0.3228	0.3071	0.1959	0.2423
PDMS-P4	0.1332–0.1660 (288–328 K)	0.2417	0.2318	0.2408	0.2580	–	–

TABLE II s values of dark conduction and s' values of photoconduction in PDMS-P2 and PDMS-P4

Compound	s values of dark conduction	s' values of photoconduction					
		100%	63%	52%	29%	Visible only	u.v. only
PDMS-P2	0.9918	0.9858	0.9794	0.9622	0.9712	0.9698	0.9744
PDMS-P4	0.9846	0.9649	0.9905	0.9838	0.9746	0.9843	0.9371

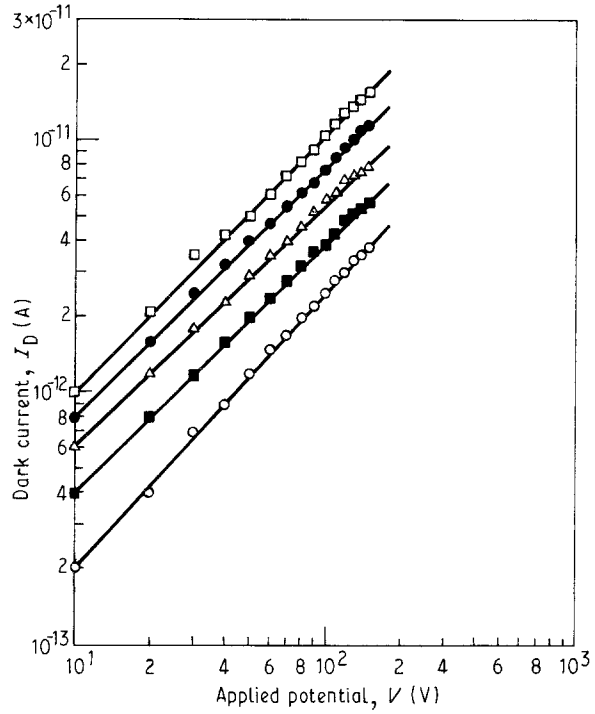

Figure 6 Dependence of dark current on applied potential (or field strength) in PDMS-P2 at different temperatures: (○) 288, (■) 298, (△) 308, (●) 318, and (□) 328 K.

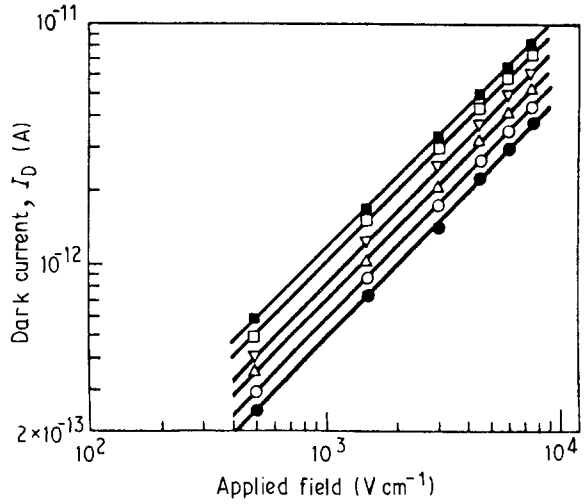

Figure 7 Dependence of dark current on applied potential (or field strength) in PDMS-P4, at different sample temperatures: (●) 288, (○) 298, (▽) 308, (△) 318, (□) 328, and (■) 332 K.

against the applied potential (field), the values of s can be evaluated.

The parameter $s \simeq 1$ for both the compounds, which has been observed at the potentials used for the measurement of the current up to the temperature range studied, clearly points at the ohmic conductivity and the observed current is due to the thermally generated charge carriers. Therefore, injection of charge carriers from the electrode does not seem to be present.

It is seen from Figs. 6 and 7 that the dark current of both the compounds in the present discussion range between 10^{-13} to 10^{-11} A. The low conductivity is possibly due to a relatively broad forbidden zone between the valance band and the conduction band. The thermally excited charge carriers are very low in number and the conductivity might be due to the influence of the iodide anion acting as donor impurity. This can be declared from the fact that some charge transfer interaction is present between the dye cation and the iodide anion in the case of 1,1′-diethyl 2,2′-thiocarbocyanine iodide [20] and the same is expected to be present in the compounds under discussion.

3.2. Photoconductivity

Analogous to phthalocyanines [37, 38] and cationic dyes [22–24], the photoconductivity of PDMS-P2 and PDMS-P4 increases rapidly (within 1 second) on irradiation with light radiation, of which, the visible part is more effective in inducing an appreciable

photocurrent compared to its u.v. counterpart. In discussing the photoresponse of PDMS-P2 and PDMS-P4, the following relationships should be taken into account:

1. The surface-type photocell was irradiated through the dye surface. Figs 8 and 9 represent the dependence of photocurrent (I_{ph}) on the light intensity (I_B). The photocurrent increases with the increasing light intensity according to the relation

$$I_{ph} = bI_B^{\gamma} \quad (3)$$

where b is a constant and γ is the intensity parameter.

For PDMS-P2 and PDMS-P4, with polychromatic light from the 500 W xenon arc lamp, the values of the intensity parameter γ ranges between 0.637–1.0283 for PDMS-P2 and has values between 1.7425–2.1778 for PDMS-P4. In both compounds, the γ values increase with increasing applied potential. This type of intensity dependence of photocurrent is evidently due to the presence of several defect states that control the charge carrier recombination [39, 40]. The results also show that the photogeneration process is one photon process. With the change of applied potential, the value of γ changes slightly. In PDMS-P2 at 10 V the value of γ is 0.8215 and at 150 V it increases to 0.7942, the sample temperature being 288 K. Similarly, at 328 K, the value of γ for 10 V is 0.6725 and it increases to 1.0283 at 150 V. This change might be due to the presence of a potential barrier, which is lowered by the increase in applied potential. Due to the decrease of the potential barrier the electron concentration in the depletion region decreases. The rate of recombination then becomes less important compared to the rate of trapping. Thus the dependence of I_{ph} on I_B may be expected to change from a sublinear to a linear dependence with increasing field [41]. Pal *et al.* [42] also report a similar change-over from a square root dependence to a linear dependence with increasing applied field in Astacin sandwich cells.

In the case of PDMS-P4, we observe values for γ greater than 1, showing a superlinear dependence of photocurrent with respect to the intensity. In other words, the photocurrent grows faster than the increase in the light intensity. The superlinear dependence of photocurrent on the light intensity may be due to the influence of several defect states with different electronic behaviour. The electron and the hole concentration, which grow with the light intensity, shift their quasi-fermi level towards the conduction and valance band, respectively. Following a series of subsequent steps, the original recombination centres are replaced by the defect centres produced by electronic doping, which eventually leads to an increase in the photocurrent more strongly than that expected from a linear dependence. The value of $\gamma = 2$ observed for PDMS-P4 results, where the bimolecular recombination of the carriers produced by singlet excitons is negligible.

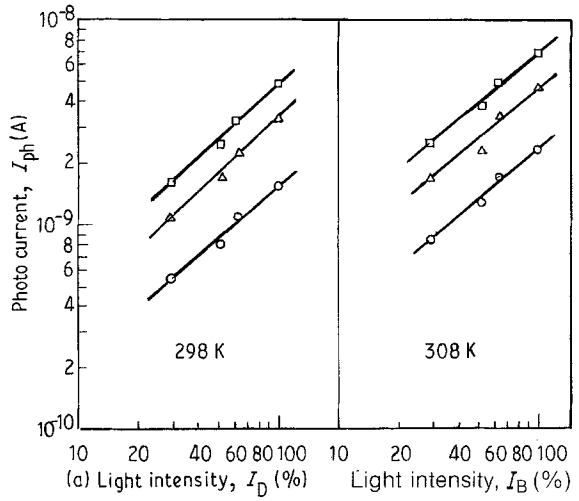

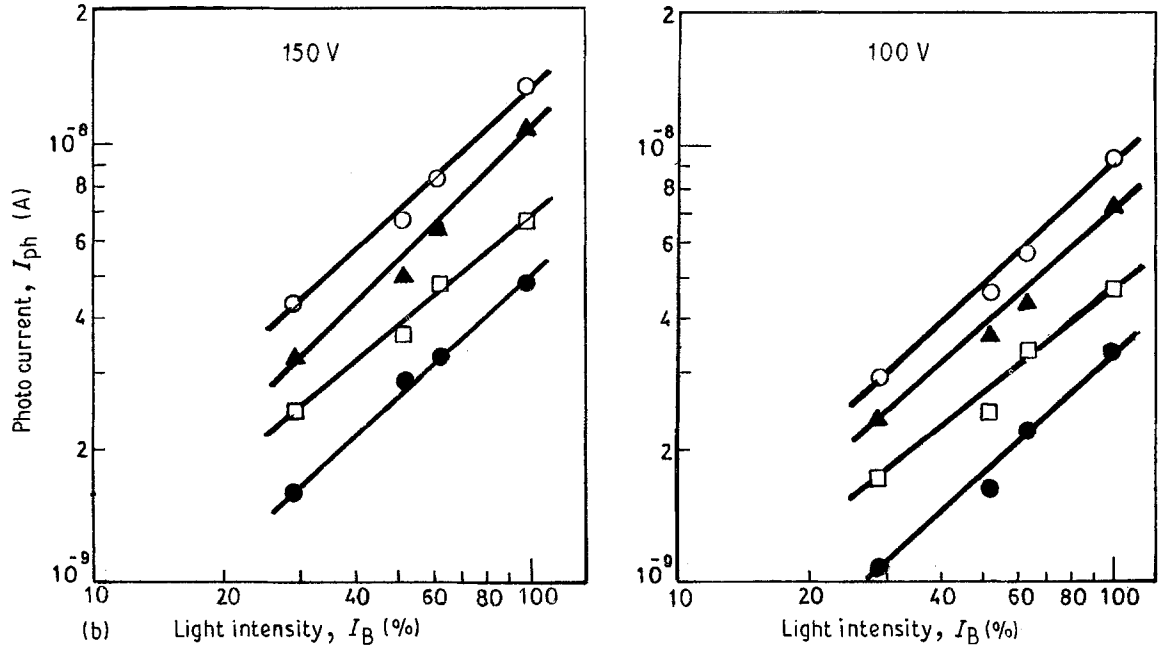

Figure 8 Dependence of photocurrent on light intensity in PDMS-P2. The sample temperature and the applied potential at which it is drawn are given. I_B (unfiltered; 100%) 12 mW/sample. (a) at different applied potentials. (○) 50, (△) 100 and (□) 150 V; (b) at different temperatures: (●) 298, (□) 308, (▲) 318, and (○) 328 K.

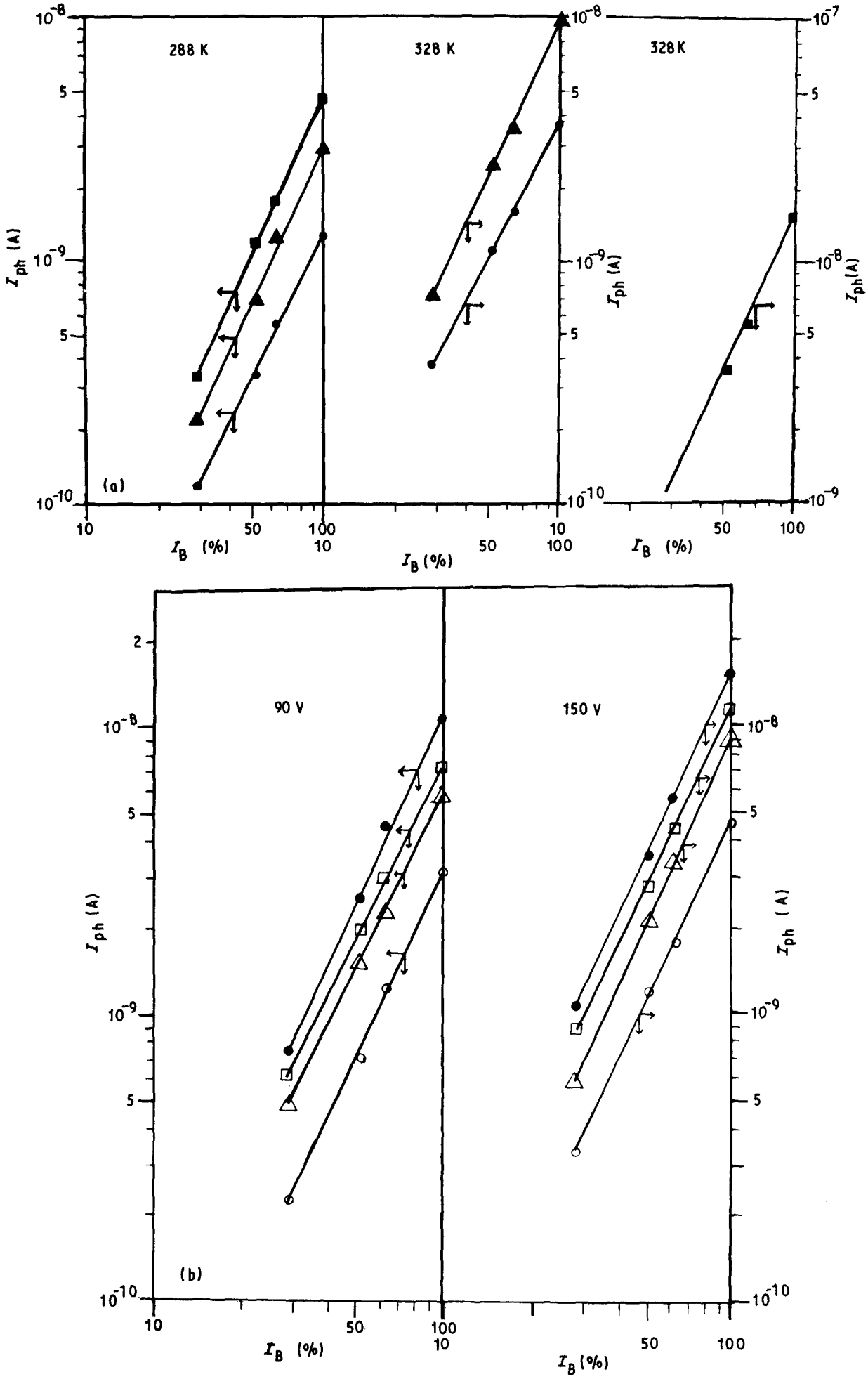

Figure 9 Dependence of photocurrent on light intensity in PDMS-P4. I_B (unfiltered; 100%) 12 mW/sample. (a) at different applied potentials: (■) 150, (▲) 90, and (●) 30 V. (b) at different temperatures: (●) 328, (□) 318, (△) 308, and (○) 288 K.

2. The photocurrents increase with the increasing voltage (field), according to the relation

$$I_{ph} = a'U^{s} \quad (4)$$

where a' is constant and s' is the power factor, the values of which are given in Table II. Plots of the logarithm of photocurrent against the logarithm of the applied potential (field), for the two compounds are shown in Figs 10 and 11. The parameter $s' = 0.9618 - 1.0023$ for PDMS-P2 and $s' = 0.87 - 0.99$ for PDMS-P4 is well within the agreeable limits of the ohmic character of the photocurrent.

3. The presence of oxygen quenches the photoconductivity, and the observed photocurrents were orders of magnitude lower in the presence of oxygen than that *in vacuo* for PDMS-P2 and PDMS-P4. Hence, both PDMS-P2 and PDMS-P4 can be characterized as n-type semiconductors [43], which is in agreement with the predictions of Nelson [22] that cationic dyes are n-type semiconductors.

4. The estimation of the photoconductive gain G, defined as the number of charge carriers passing through the sample per absorbed photon [2], according to the equation

$$G = \frac{I_{ph}/e}{I_A V} \quad (5)$$

where I_{ph} is the photocurrent at a particular wavelength, applied field and temperature, e is the electronic charge, I_A is the number of photons absorbed by the sample and V is the volume of the sample, gives the value of G ($\lambda \doteq 472$ nm, $U = 1500\ \mathrm{V\,cm^{-1}}$ and $T = 328$ K) approximately as 6.05×10^{-4} for PDMS-P2 and 8.6×10^{-4} for PDMS-P4. Comparing these values with those values already reported by Meier [38, 44], by Dalburg and Musser [25, 26] and Chamberlin [27], PDMS-P2 and

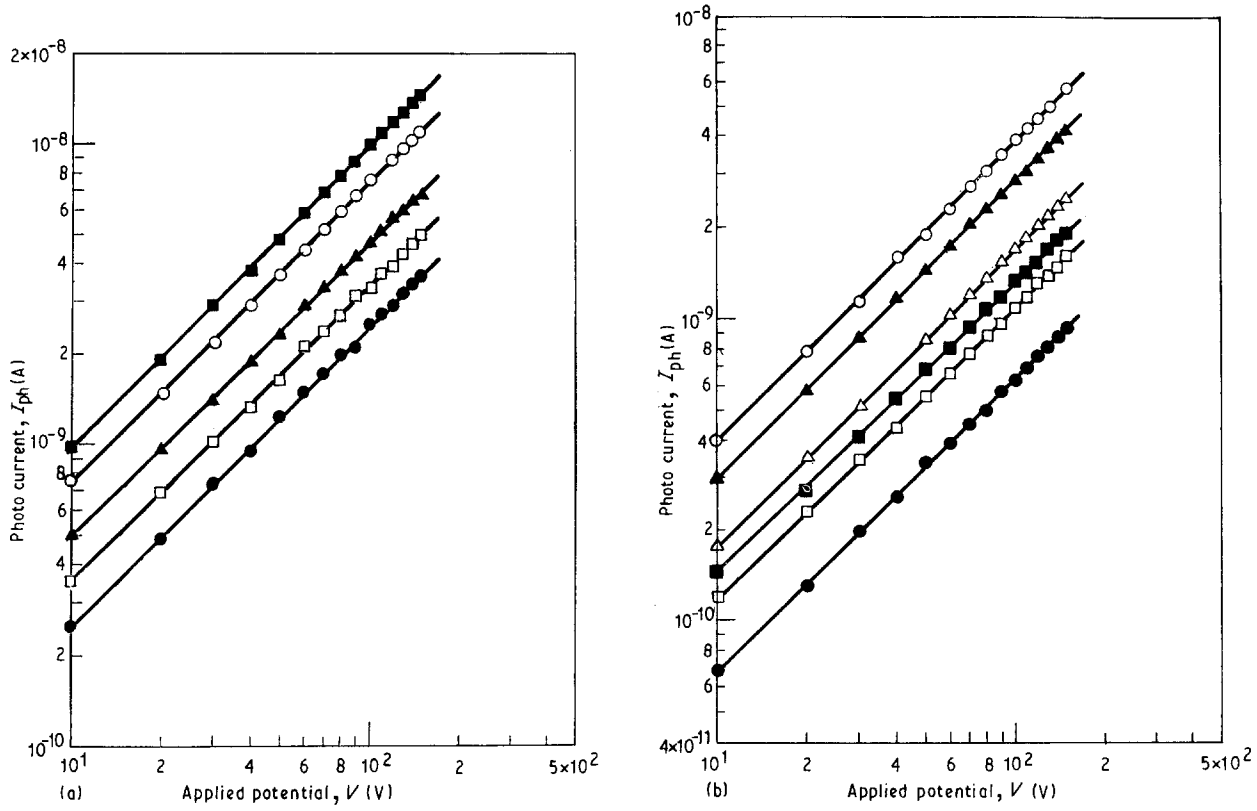

Figure 10 Dependence of photocurrent on applied potential (field) in PDMS-P2. I_B (unfiltered 100%). 12 mW/sample. (a) for 100% intensity at temperatures: (●) 288, (□) 298, (▲) 308, (○) 318, and (■) 328 K; (b) for 29% intensity at (●) 288, (□) 298, (■) 308 K, and for 52% intensity at (△) 308, (▲) 318, (○) 328 K.

TABLE III r values of photoconduction and the dark current and photocurrent maxima in PDMS-P2 and PDMS-P4. The temperature and the applied potentials at which the values are obtained are given in parenthesis

Compound	Value of γ	Dark current maxima (10^{-12} A)	Photocurrent maxima (10^{-9} A)					
			100%	63%	52%	29%	Visible	u.v.
PDMS-P2	0.9635–0.7835	17.14 (150 V, 332 K)	14.83 (150 V, 332 K)	8.45 (150 V, 332 K)	5.75 (150 V, 323 K)	4.41 (150 V, 323 K)	1.21 (150 V, 323 K)	0.78 (150 V, 323 K)
PDMS-P4	1.8705–2.1973	8.5 (150 V, 328 K)	16.31 (150 V, 328 K)	6.1 (150 V, 328 K)	4.25 (150 V, 328 K)	1.175 (150 V, 328 K)	4.09 (150 V, 328 K)	1.02 (150 V, 328 K)

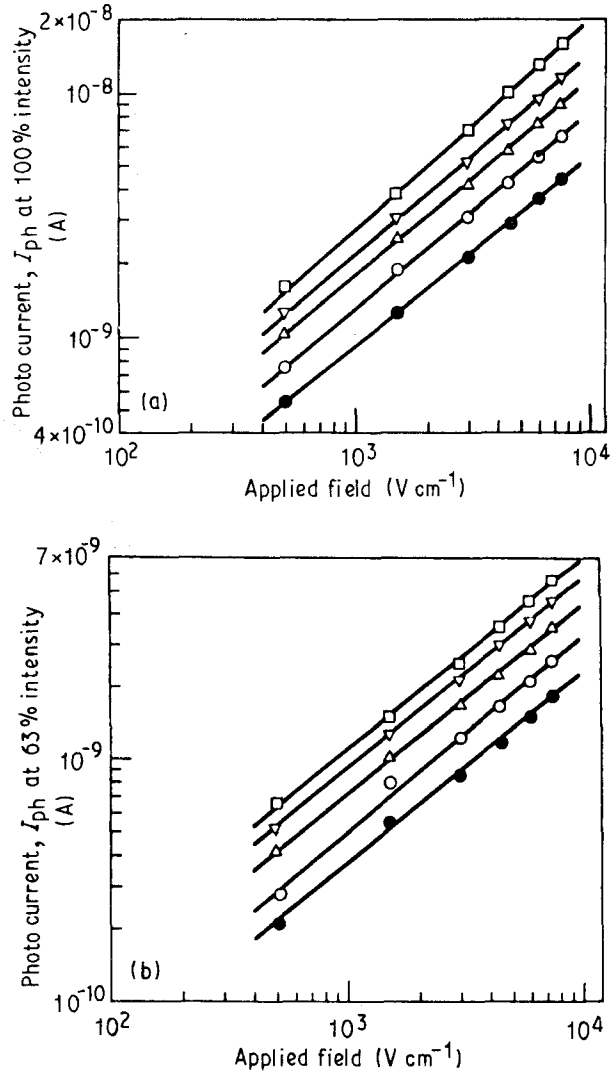

Figure 11 Dependence of photocurrent on applied potential (field) in PDMS-P4. I_B (unfiltered 100%). 12 mW/sample. (a) at 100% intensity and (b) at 63% intensity, for different temperatures: (●) 288, (○) 298, (△) 308, (▽) 318, and (□) 328 K.

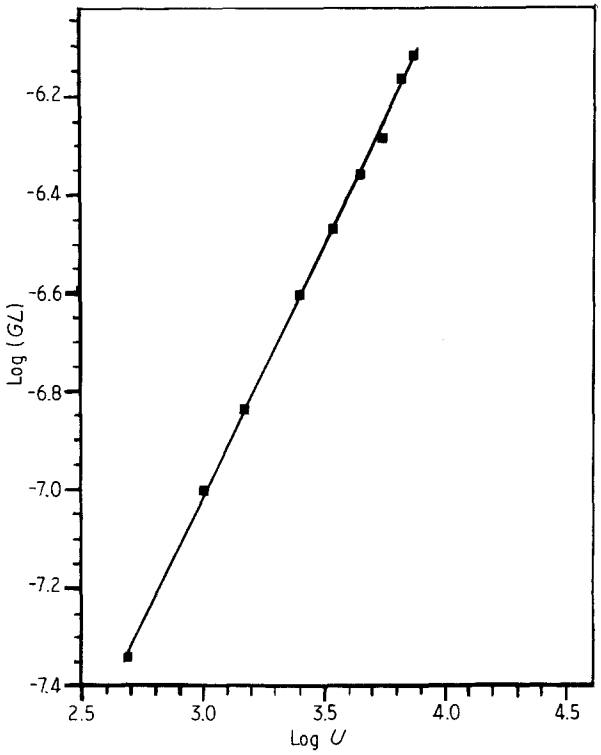

Figure 12 Plot of the product of the photoconductive gain (G) and the distance between two successive electrodes (L) against the applied field (U) for PDMS-P2 at 472 nm and $T = 328$ K. $I_A = 3 \times 10^{11}$ photons cm^{-2}S^{-1}.

PDMS-P4 can be considered as organic photoconductors with moderately good photoelectric sensitivity.

For steady state photocurrents we can give the photocurrent equation as

$$I_{ph} = (e\eta I_A V\mu\tau U/L)(1 - \exp(-L/\mu\tau U)) \quad (6)$$

where U is the field strength, L is the distance between the electrodes, μ is the mobility, τ is the carrier life time and η is the quantum efficiency of carrier generation. Taking $\mu\tau U \ll L$ (which shall be proved later), Equation 6 can be rewritten

$$G = \eta\mu\tau U/L \quad (7)$$

Logging both sides of Equation 7 gives

$$\log GL = \log \eta\mu\tau + z \log U \quad (8)$$

where z is a constant.

A logarithmic plot of the product of the gain and the electrode distance against the field is shown in Fig. 12 and is linear.

If we take into consideration, the field dependence of the gain, the mean distance of the carrier drift (given as Schubweg, $\mu\tau U$, carrier range $\mu\tau$) can be derived from the above plot. The parameters derived from the above plot are given in Table IV.

Additional information may be derived from a study of the intensity and temperature-dependence of photocurrents.

The sublinear intensity-dependence of the photocurrent density (J_{ph}) in the ohmic region [39] for PDMB-P2 can be given by the equation

$$J_{ph} = (e\mu U/L)[(f/vsH)^{Tc/(Tc+T)}][N_C^{(T/Tc+T)}] \quad (9)$$

where e is the electronic charge, f is the number of excitations per cm^3, v is the thermal velocity, s is the capture cross section of the carriers, H is the volume

TABLE IV The values of photoconductive gain (G), the carrier life-time (τ), the Schubweg ($\mu\tau U$), and carrier range ($\mu\tau$), value of z (Equation 8) in PDMS-P2 and PDMS-P4. The value of Schubweg is calculated at a field $U = 5 \times 10^3$ V cm^{-1} at $\lambda = 472$ nm

Compound	Photoconductive gain, G ($\times 10^{-4}$)	Schubweg*, $\mu\tau U$ ($10^{-4} \times$ cm^{-2})	Carrier range, $\mu\tau$ ($10^{-8} \times$ cm^{-2}V^{-1})	Value of z
PDMS-P2	6.05	2.4984	4.9967 ($T = 328$ K, $\lambda = 472$ nm)	1.03125
PDMS-P4	8.60	–	–	

density of trapping states and N_C is the effective density of states.

Equation 9 can be rewritten:

$$\dot{J}_{ph} = (f/vsH)[N_C^{(T/Tc)}] \quad (10)$$

where $\dot{J}_{ph} = (\dot{J}_{ph} \times L/e\mu U)^{(Tc+T)/Tc}$.

Logging both sides of Equation 10:

$$\log \dot{J}_{ph} = \log f/vsH + [(T/T_C)\log N_C] \quad (11)$$

A plot of $\log \dot{J}_{ph}$ against T/T_C would give the effective density of states N_C from the slope and the value of the carrier life time τ $(= 1/vsH)$ from the intercept (Fig. 13).

The following values of N_C and f/vsH could then be obtained: $N_C = 1.2712 \times 10^{11}$, which is in agreement with the characteristic density of states for wide band semiconductors [11, 30] and $f/vsH = 1.1258 \times 10^8$, from which the value of the carrier life time can be calculated. The value of τ obtained from the above relation is $= 3.75266 \times 10^{-8}$, which is lower than that estimated from Equation 8.

5. The temperature dependence of photocurrent can be given by

$$I_{ph} = A' \exp(-\Delta E_{ph}/kT) \quad (12)$$

where A' is the pre-exponential factor and ΔE_{ph} is the activation energy of photoconduction. From the plots of $\log I_{ph}$ against $1/T$ (Figs 14 and 15), the value of ΔE_{ph} could be calculated and the values of ΔE_{ph} are given in Table I. The value of ΔE_{ph} ranges between 0.270–0.32 for PDMS-P2 and between 0.231–0.258 for PDMS-P4. The difference in the activation energies in the dark and under illumination is evidently due to the change in the charge carrier density and its distribution in different energy states and traps after illumination. Alternatively, the activation energy of photoconduction is the energy needed for the production of the excitons and may be either the energy difference between the transport band edge and the highest exciton level or just the depth of the traps.

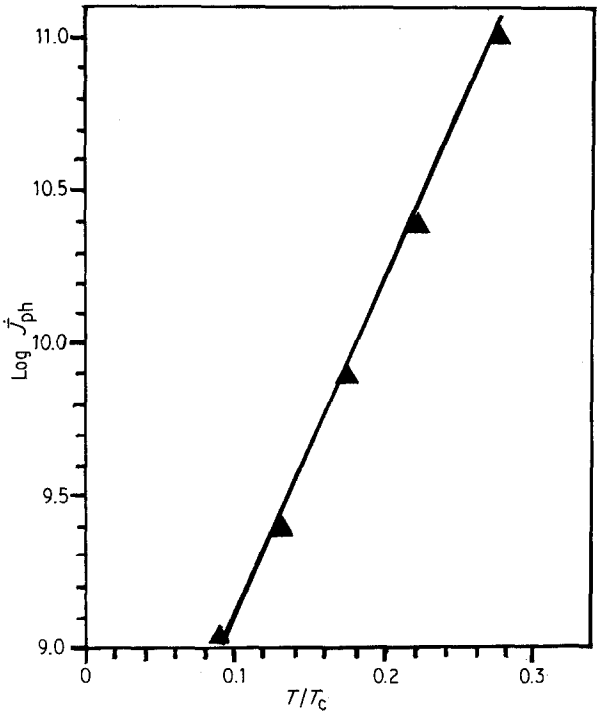

Figure 13 Plot of $\log J_{ph}$ against T/T_C. (T_C is the characteristic temperature). $L = 0.02$ cm. $V = 100$ V. $\mu = 0.01$ cm^2 V^{-1} s^{-1}.

6. A typical rise and decay transient of photocurrent consists of an initial steep rise to the maximum followed by a plateau and a steep decay followed by a tail. The shape and the reproducibility of the transients were found to depend critically on the purity of the compound and the sample preparation. Samples prepared in a vacuum of less than 10^{-4} torr showed varying levels of darkconductivity and dispersion of transients. By contrast, when the samples were prepared in a vacuum better than 10^{-4} torr and studied in a vacuum better than 10^{-5} torr, after proper degassing, highly reproducible results could be obtained. The rise time for PDMS-P2 and PDMS-P4 are of the order of one second and their decay times are of the order of 2–3 s. These values are in good agreement with the values reported by Nelson for cationic dyes [22–24]. The rise and decay times of this order clearly suggest the presence of traps in the forbidden zone. The possibility of charge carrier injection from the electrodes is ruled out. This is evident from the steady state I_{ph} against V characteristics shown in Figs 10 and 11. The decrease in the rise and decay times with increasing temperature lends support to the thermal release of the charge carriers from the traps. Further experiments using the time of flight technique (TOF) to measure the drift mobilities would throw more light on this fact.

The rise and decay transients were reproducible, but their reproducibility below 10^3 V cm^{-1} was not satisfactory. No measurable change in the rise and decay time with increasing electric field could be observed, which clearly indicates that the drift velocity ($v = \mu U$) is independent of the field. This result can be verified from the TOF experiments. The relatively long tail may result because of a small fraction of the charge carriers getting localized for a relatively long period in the traps.

The near-rectangular transients (Figs 16 and 17) reported here indicate a narrow charge dispersion compared with what is typically reported in the literature [30]. Because of the narrow dispersion, the transients can more clearly be demonstrated and analysed in the linear current I_{ph} against the time scale, instead of the usual plots of $\log I_{ph}$ against $\log t$. The transients clearly indicate a second order kinetics.

The transients recorded under a variety of conditions can be analysed by comparing the normalised current shapes. The current I_{ph} is normalised to its initial value I'_{ph} (maximum value) in the plateau region and the time t is normalised to its value $t_{1/2}$, which is the time when the current drops to half of I'_{ph} (defined as the transit time) (see Fig. 18). This method normalises the overall numbers of the carriers and the transit time of the charge distribution peak. The length of the normalised current tail then reflects the ratio of the spacial spread of the charge packets to its mean position and is then defined as a measure of the relative dispersion of the transisting carriers.

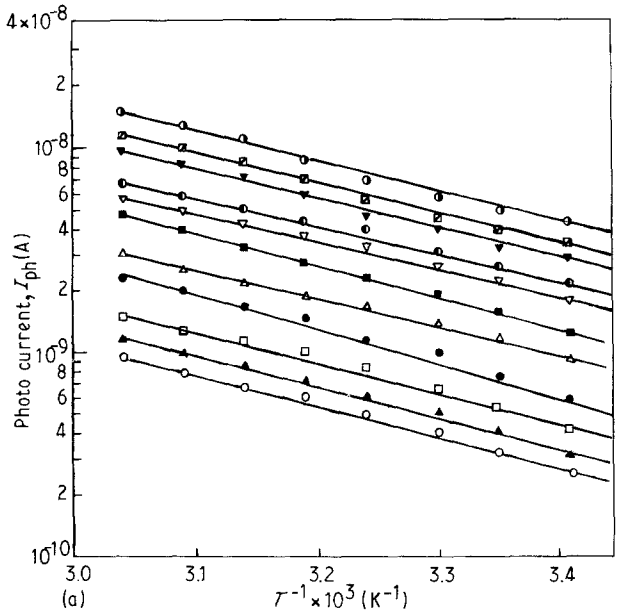

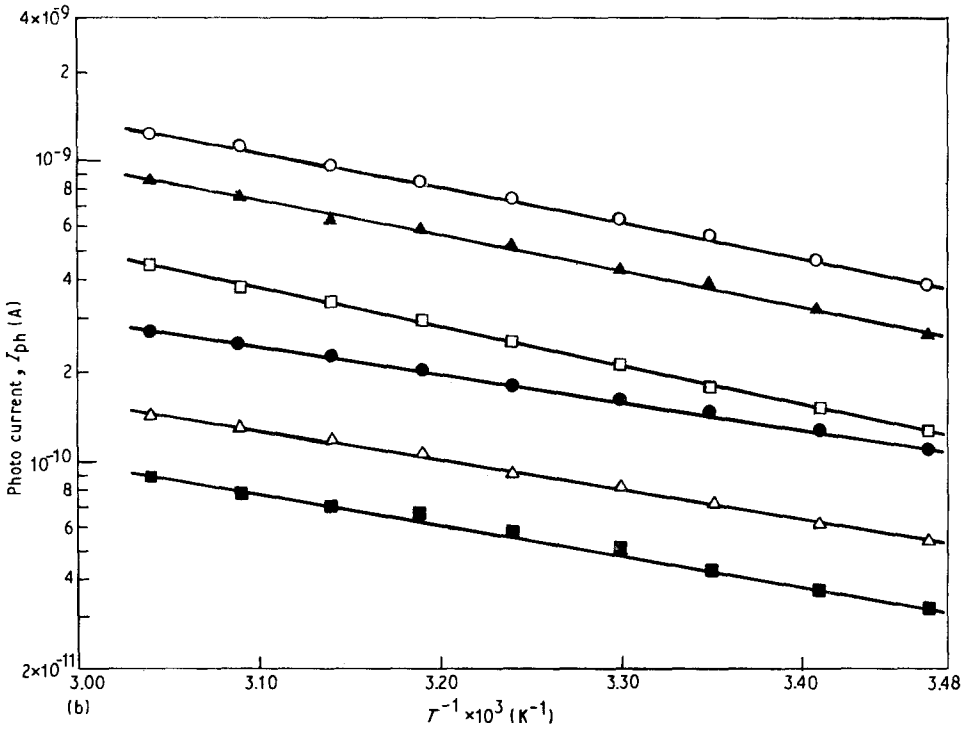

Figure 14 Temperature dependence of photocurrent on applied potential in PDMS-P2 surface cell. $L = 0.02$ cm. (a) At different illuminations, I_B: (○) 29% (30 V), (□) 29% (50 V), (▲) 52% (30 V), (●) 52% (60 V), (■) 52% (120 V), (△) 63% (50 V), (▽) 63% (100 V), (◐) 63% (120 V), (▼) 100% (100 V), (⊠) 100% (120 V), and (◑) 100% (150 V). (b) at $\lambda = 472$ nm (visible radiation): (○) 150, (▲) 100, (□) 50 V and at $\lambda = 337$ nm (u.v. illumination): (●) 100, (△) 50, (■) 30 V.

TABLE V Values of the photocurrent rise and decay times, the open circuit photovoltage (V_{oc}), the short circuit photocurrent (I_{sc}), the absorption maxima and the ratio of the photocurrent to darkcurrent observed in PDMS-P2 and PDMS-P4. The absorption spectra were recorded in spectral grade methanol

Compound	Photocurrent Rise time (s)	Decay time (s)	V_{oc} (mV)	I_{sc} (nA)	Absorption maximum (nm)	I_{ph}/I_D
PDMS-P2	0.65–0.8	1.0–3.0	73.0	0.34	475	80–125
PDMS-P4	1.0–2.0	1.5–3.0	1270	0.88	470	1725–2000

7. It has been shown that a relationship exists between the number of laws governing the conductivity of the dyes and their spectral sensitization properties. A dye can be a suitable sensitizer of a photoconductor, *viz.* silver halide, which is capable of being strongly adsorbed by the latter and an interchange of charge carriers is physically possible [45, 46]. PDMS-P4 shows a higher photoconductivity compared to

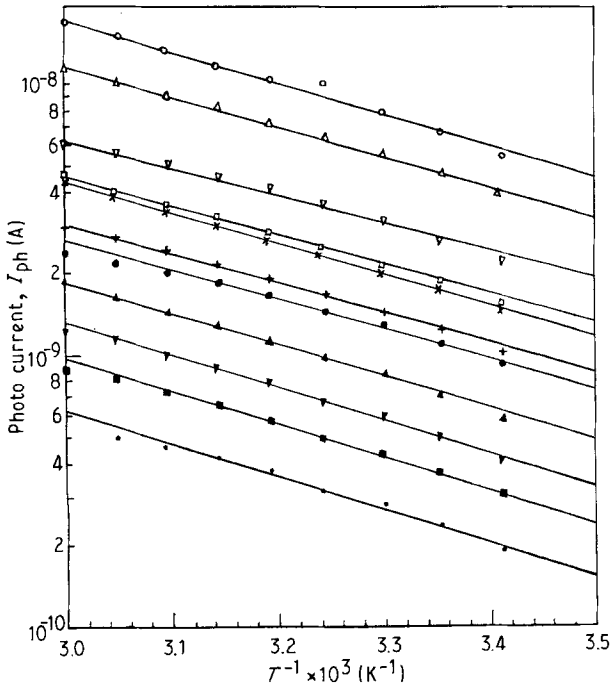

Figure 15 Temperature dependence of photocurrent on applied potential in PDMS-P4 surface cell. $L = 0.02$ cm. At different intensities of illuminations: I_B: (▽) 100% (50 V), (△) 100% (100 V), (○) 100% (150 V), (●) 63% (50 V), (□) 63% (100 V), (▲) 52% (50 V), (+) 52% (100 V), (×) 52% (150 V), (●) 29% (50 V), (■) 29% (100 V), (▼) 29% (150 V).

PDMS-P2, and is found to be a strong sensitizer [47]. The planarity of the molecule which is a precursor for a good photosensitizer [45, 46, 48] supports the result.

8. Photovoltaic effect is characterized by the appearance of a photoelectric potential and current in the absence of an applied potential. Maximum open circuit photovoltage (V_{oc}) and short circuit photocurrent (I_{sc}) have been measured and the values clearly indicate that PDMS-P2 and PDMS-P4 can be used in solar photovoltaic devices with good efficiencies (Table IV).

9. The absorption spectra of PDMS-P2 and PDMS-P4 were recorded in methanol. Both PDMS-P2 and PDMS-P4 showed a high extinction coefficient in the visible region. To study the effect of u.v. and visible radiations separately on the photoconduction of the compounds, visible and u.v. cut-off filters were used. Both the compounds showed a higher photoconduction on illumination with visible radiation, which augments the higher extinction coefficients observed in the compounds.

Accordingly with a good photoconductive gain, higher photoconductivity in the visible part of the solar spectrum and a good sensitizing effect, the listed compounds can be considered a potential candidate

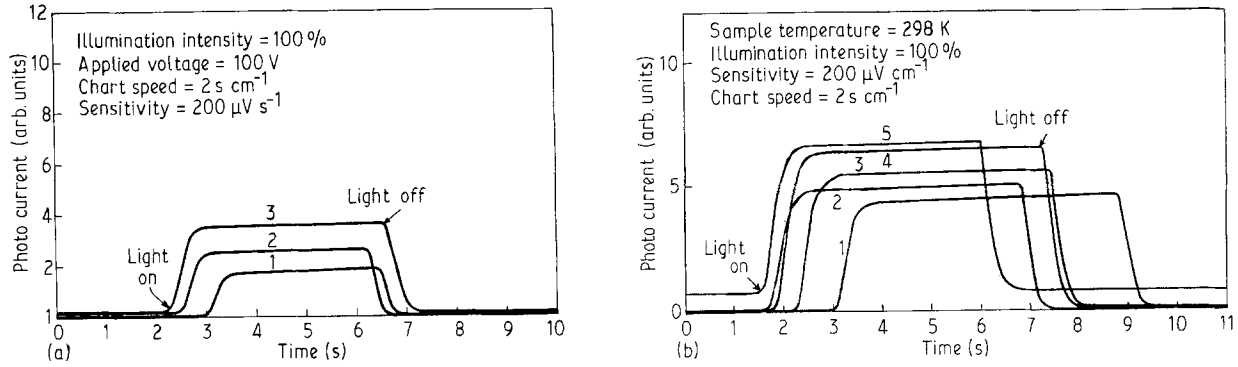

Figure 16 Photocurrent transients (rise and decay time curves) for PDMS-P2 (a) at different temperatures: (1) 303, (2) 308, and (3) 318 K; and (b) at different applied potentials: (1) 50, (2) 75, (3) 100, (4) 125 and (5) 150 V. I_B, 12 mW/sample, unfiltered.

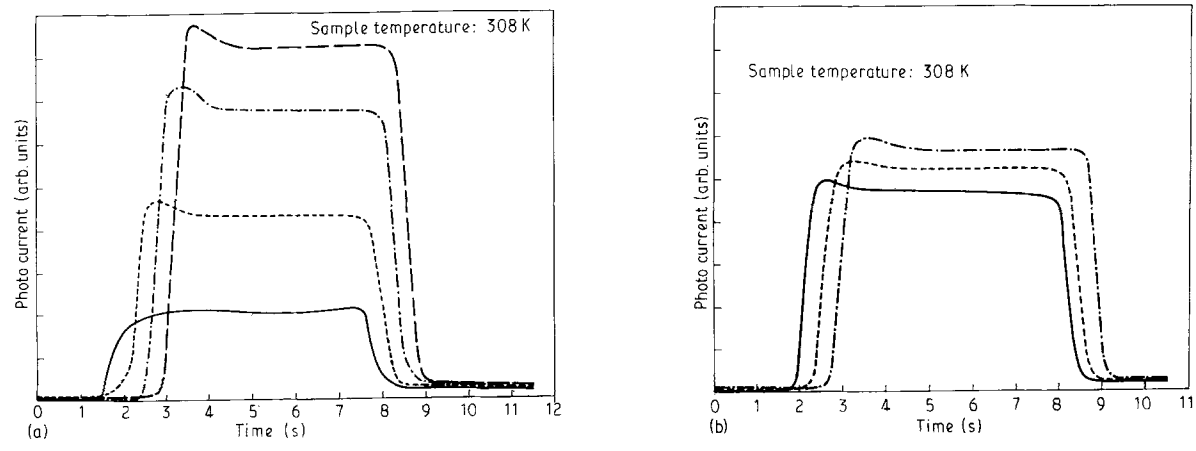

Figure 17 Photocurrent transients (rise and decay time curves) for PDMS-P4 at different applied potentials. (a) (——) 0, (– – –) 1, (—·—·—) 25, and (————) 50 V; and for (b) (——) 100, (– – –) 125, and (—·—·—) 150 V. I_B, 12 mW/sample, unfiltered.

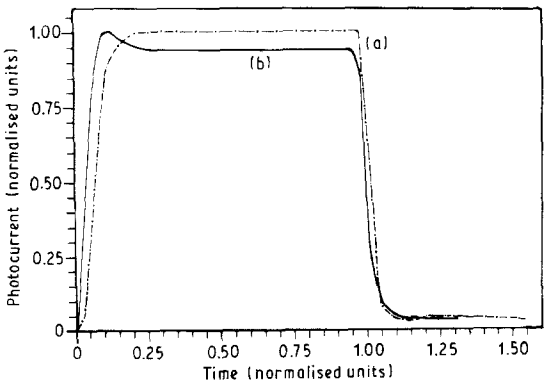

Figure 18 A plot of the normalised photocurrent transient for (a) PDMS-P2 (308 K, 100 V, 100%) and (b) PDMS-P4 (298 K, 150 V, 100%). The curves are the normalised transients of Fig. 17. For the definition of normalisation, see text.

for solar photovoltaics with reasonably good conversion efficiencies.

4. Conclusion

In summary, the following conclusions can be drawn:

1. The dark and photocurrent dependence on the applied field and temperature suggests that discrete trapping levels are involved in the charge carrier generation and the dominant trapping levels are different for dark and photoconduction.
2. The study of the intensity dependence of photoconduction, clearly points out that the photogeneration of charge carriers is one photon process, but is trap-limited and the charge carrier generation is by excitons. The mobility being field-independent, there is at least one kinetically important process which is field-dependent; it may either be the detrapping of the charge carriers from the occupied traps or the decrease in the rate of recombination of the charge carriers with increasing fields.
3. The charge carrier transport can be explained on the basis of band model with different trap levels in the forbidden zone.
4. The results presented in this paper indicate a reasonably good photoelectric sensitivity for PDMS-P2 and PDMS-P4. In sandwich type photoresistance cells under the influence of moderately high ($\sim 10^5$ V cm^{-1}) field strengths, photocurrents in the order of a few microamperes can be achieved.

Acknowledgements

Two of the authors (PKNR and HOY) are grateful to the University Grants Commission of India for the award of fellowships under the Centre of Advanced Studies Scheme. One of us (PKNR) is particularly thankful to the Chemical Engineering Faculty of the Department of Chemical Technology at University of Bombay for sparing their computer facilities and for S. C. Mathur at the Physics Department of the Indian Institute of Technology, New Delhi for his suggestions. Two of the authors (LNP and SD) are indebted to the Council of Scientific and Industrial Research, India, for its financial support.

References

1. F. H. MOSES and A. L. THOMAS, "Phthalocyanine Compounds" (Rhenold, New York, 1963).
2. H. MEIER, *Topics in Current Chemistry* **61** (1976) 87.
3. J. W. WEIGL, *Angew. Chem.* **89** (1977) 386.
4. S. NAKAMURA, T. OZAKI, K. TORIYAMA, K. IIDA and G. SAWA, *Jap. J. Appl. Phys.* **81** (1989) 991.
5. J. P. LAUNARY, M. SOWINSKA, L. LEYDIER and A. GOURDON, *Chem. Phys. Lett.* **160** (1989) 89.
6. H. MEIER, U. TSCHIRWITZ, E. ZIMMERHACKL, W. ALBRECHT and G. ZEITLER, *J. Phys. Chem.* **81** (1977) 712.
7. H. MEIER, W. ALBRECHT, U. TSCHIRWITZ, N. GEHEEB and E. ZIMMERHACKL, *Ber. Bunsenges. Phys. Chem.* **81** (1977) 592.
8. T. KLOFTA, C. LINKONS and N. R. ARMSTRONG, *J. Elecktroanal. Chem.* **185** (1985) 73.
9. H. MEIER and W. ALBRECHT, *Ber. Bunsenge. Phys. Chem.* **73** (1969) 86.
10. A. T. TWAROWSKI, *J. Chem. Phys.* **76** (1982) 2640.
11. H. MEIER, "Organic Semiconductors: Dark and photoconductivity of organic solids" (Verlag Chemie, Weinheim, 1974).
12. F. R. FAN and L. R. FAULKNER, *J. Chem. Phys.* **69** (1978) 3341.
13. M. MARTIN, J. J. ANDRE and J. SIMON, *J. Appl. Phys.* **54** (1983) 2792.
14. M. SHIMURA and A. TOYODA, *Jap. J. Appl. Phys.* **23** (1984) 1462.
15. J. H. PERLSTEIN, in "Electrical properties of polymers", edited by D. A. Seanor (Academic Press, London, 1982).
16. K. KUDO and T. MORIIZUMI, *Jap. J. Appl. Phys.* **20** (1981) L553.
17. F. GALLUZZI, *J. Phys. D: Appl. Phys.* **18** (1985) 685.
18. M. TOMIDA, S. KUSABAYASHI and M. YOKOYAMA, *Chem. Lett.* (1984) 1305.
19. M. Q. DOJA and D. PRASAD, *Ind. J. Chem. Soc.* **20** (1943) 153.
20. N. KAZUMI, H. YOSHIOKA and H. MOROSHITA, *Acta Cryst.* **B-33** (1977) 2181.
21. P. J. WHEATLEY, *J. Chem. Soc.* (1959) 3245.
22. R. C. NELSON, *J. Chem. Phys.* **22** (1955) 885.
23. *Idem., ibid.* **23** (1955) 1550.
24. *Idem., J. Opt. Soc. Amer.* **50** (1960) 1029.
25. S. C. DAHLBERG and M. E. MUSSER, *J. Chem. Phys.* **70** (1979) 5021.
26. *Idem., ibid.* **71** (1979) 2806.
27. G. A. CHAMBERLEIN, *Nature* **289** (1981) 45.
28. P. YAMIN, *J. Phys. Chem.* **86** (1982) 3796.
29. J. MOTT and N. L. JARVIS, *J. Amer. Chem. Soc.* **106** (1984) 4706.
30. F. GUTMAN and L. E. LYONS, "Organic Semiconductors" (Wiley & Sons, New York, 1967) p. 117.
31. Z. R. GRABOWSKI, K. ROTKIEWICZ, A. SIEMIAVCZUK, D. J. COWLEY and W. BAUMANN, *Nouv. J. Chim.* **3** (1979) 443.
32. W. RETTIG, *Angew. Chem. Intern. Ed.* **25** (1986) 971.
33. E. LIPPERT, W. RETTIG, V. BONACIC-KOUTECKY, F. HEISEL and J. MEIHE, *Adv. Chem. Phys.* **68** (1987) 1.
34. M. SOWINSKA, J. LAUNAY, J. MUGNIER, J. POUGET and B. VALEUR, *J. Photochem.* **37** (1987) 69.
35. L. N. PATNAIK and S. DAS, *Tetrahedron Lett.* **21** (1985) 4961.
36. P. K. NARASIMHARAGHAVAN, Ph.D. Thesis, Bombay University (1987).
37. H. MEIEI, W. ALBRECHT, D. WOHRLE and A. JAHN, *J. Phys. Chem.* **90** (1986) 6349.
38. H. MEIER, W. ALBRECHT, E. ZIMMERHACKL, M. HANACK and J. METZ, *Syn. Met.* **11** (1985) 333.
39. A. ROSE, "Concepts in Photoconductivity and Allied Problems" (Interscience, New York, 1963).

40. F. STOCKMANN, *Phys. Stat. Solidi* **34** (1969) 741.
41. L. V. AZARRAGA, Ph.D. Thesis, Lousiana State University (1964).
42. P. PAL, D. GOSH and T. N. MISHRA, *J. Phys. Soc. Jap.* **57** (1988) 1006.
43. H. MEIER, "Die Photochemie der Organischen Fabstoffe" (Springer-Verlag, Berlin, 1963) p. 173.
44. H. MEIER and W. ALBRECHT, *Z. Phys. Chem. Neue Folge Bd.* **148** (1986) 171.
45. R. O. LOUTFY, B. S. ONG and J. JADROS, *J. Imag. Sci.* **29** (1985) 69.
46. F. M. HAMER, *J. Chem. Soc.* (1956) 1480.
47. F. M. HAMER, in "The Cyanine Dyes and related Compounds" (Interscience, 1964) p. 438.
48. L. N. PATNAIK, Personal Communications.

Received 25 May
and accepted 24 October 1990